Conference paper: International Workshop on Recent Advances in Monte Carlo Techniques for Radiation Therapy, Montreal, Canada, June 2011.

Monte Carlo verification of gel dosimetry measurements for stereotactic radiotherapy‡

T. Kairn[1], M. L. Taylor[2], S. B. Crowe[3], L. Dunn[2,4], R. D. Franich[2], J. Kenny[1]§, R. T. Knight[1], J. V. Trapp[3]

[1] Premion, The Wesley Medical Centre, Suite 1, 40 Chasely St, Auchenflower, Qld 4066, Australia

[2] School of Applied Sciences and Health Innovation Research Institute, RMIT, Melbourne Vic 3001, Australia

[3] Faculty of Science and Technology, Queensland University of Technology, GPO Box 2434, Brisbane Qld 4001, Australia

E-mail: kairn@physics.org

Abstract.

The quality assurance of stereotactic radiotherapy and radiosurgery treatments requires the use of small-field dose measurements that can be experimentally challenging. This study used Monte Carlo simulations to establish that PAGAT dosimetry gel can be used to provide accurate, high-resolution, three-dimensional dose measurements of stereotactic radiotherapy fields. A small cylindrical container (4 cm height, 4.2 cm diameter) was filled with PAGAT gel, placed in the parietal region inside a CIRS head phantom, and irradiated with a 12 field stereotactic radiotherapy plan. The resulting three-dimensional dose measurement was read out using an optical CT scanner and compared with the treatment planning prediction of the dose delivered to the gel during the treatment. A BEAMnrc/DOSXYZnrc simulation of this treatment was completed, to provide a standard against which the accuracy of the gel measurement could be gauged. The three dimensional dose distributions obtained from Monte Carlo and from the gel measurement were found to be in better agreement with each other than with the dose distribution provided by the treatment planning system's pencil beam calculation. Both sets of data showed close agreement with the treatment planning system's dose distribution through the centre of the irradiated volume and substantial disagreement with the treatment planning system at the penumbrae. The Monte Carlo calculations and gel measurements both indicated that the treated volume was up to 3 mm narrower, with steeper penumbrae and more variable out-of-field dose, than predicted by the treatment planning system. The Monte Carlo simulations allowed the accuracy of the PAGAT gel dosimeter to be verified in this case, allowing PAGAT gel to be utilised in the measurement of dose from stereotactic and other radiotherapy treatments, with greater confidence in the future.

‡ Experimental aspects of this work were originally presented at the Engineering and Physical Sciences in Medicine Conference (EPSM-ABEC), Melbourne, 2010.

§ Now at Australian Clinical Dosimetry Service, ARPANSA, Yallambie Vic, Australia

1. Introduction

The quality assurance of stereotactic radiotherapy and radiosurgery treatments requires the use of small-field dose measurements, for which the utility of conventional radiation dosimeters is limited (Das et al. 2008). The use of dosimetry gels has the potential to provide high-resolution measurements of dose in small fields and across steep penumbrae, without the disadvantages of volume averaging, non-water equivalence or dose perturbation that are associated with more established dosimeters (Taylor et al. 2011, Baldock et al. 2010).

Numerous authors have investigated the use of dosimetric gels for stereotactic radiotherapy dosimetry (Cosgrove et al. 2000, Pappas et al. 2001, Calcina et al. 2007, Seimenis et al. 2009). However, these studies have been limited by their use of ion chamber measurements or treatment planning calculations (derived from ion chamber measurements) to establish the accuracy of the gel measurements. In a study of Gammaknife radiosurgery dosimetry, Seimenis *et al* found that profiles measured in normoxic poly-acrylamide (PAG) gel were in good agreement with treatment planning calcultions of in-field dose, but the beam penumbrae measured in the gel were noticeably narrower than the penumbrae predicted by the treatment plan (Seimenis et al. 2009). Pappas *et al* compared stereotactic cone profiles obtained with VIPAR gel, radiographic film and an ion chamber and found that the gel gave narrower penumbrae measurements than both the film and the ion chamber (Pappas et al. 2001). Calcina *et al*'s study of Fricke xylenol gel for small, square field measurements also showed substantial differences between gel and ion chamber measurements (Calcina et al. 2007). Monte Carlo simulations have the potential to provide a standard against which the accuracy of gel dose distributions can be gauged, assisting in the commisioning of gel dosimetry systems and providing the ability of distinguish between genuine treatment plan dose errors and mis-measurement due to poor calibration (Cosgrove et al. 2000) or uncorrected physical processes withing the gel (Boudou et al. 2004).

Several authors have used Monte Carlo simulations to validate their gel measurements, but these studies have largely been limited to homogeneous cylindrical, spherical or slab phantoms (Ceberg et al. 2010, Valente et al. 2007, Guillerminet et al. 2005). Notable exceptions are Pourfallah *et al* who irradiated a vial of PAGAT gel in a purpose-built sphere phantom, containing a block heterogeneity, providing a course representation of a human head (Pourfallah et al. 2009), and Boudou *et al*, who placed a cylinder of normoxic PAG gel in a commercial head phantom and used it to study stereotactic synchrotron radiation (Boudou et al. 2007). Both studies used voxelised models of their complex phantoms to calculate Monte Carlo dose distributions for comparison with the gel measurements.

Our study, therefore, builds on the work of Pourfallah *et al* and Boudou *et al*, by using a cylinder of PAGAT gel in a heterogeneous head phantom (containing a bone-equivalent plastic skull as well as volumes of air in the nasal cavities) to evaluate a 12 field stereotactic radiosurgery treatment, designed for a 1.5 cm lesion in the brain.

In this study, the treatment plan and CT of the phantom are used to generate input data for a Monte Carlo simulation that is used to evaluate the accuracy of the dose distribution obtained from the gel. Both data sets are also compared with the dose distribution provided by our pencil-beam-based stereotactic radiotherapy treatment planninng system. This work aims to establish that PAGAT dosimetry gel can be used to provide accurate, high-resolution, three-dimensional dose measurements of stereotactic radiotherapy fields.

2. Methods

2.1. Gel irradiation

The PAGAT gel was mixed according to a recipe recommended by Venning *et al* (Venning et al. 2005), with the concentration of the oxygen scavenger (tetrakis hydroxymethyl phosphonium chloride, THPC) increased to 8mM to optimise the optical scanning result and reduce the likelihood of gel failure due to oxygen contamination (Khoei et al. 2010). PAGAT gel has been shown to be approximately equivalent to water and soft tissue, in terms of both electron density and effective atomic number (Taylor et al. 2008, Taylor et al. 2009*a*). PAGAT also exhibits a linear-dose response for doses up to 7 Gy, when MRI scanned (Venning et al. 2005, DeDeene et al. 2006) or opically scanned (Khoei et al. 2010). Our gel was set in a small (4 cm heigh, 4.2 cm diameter) cylindrical container designed for use with the CIRS head phantom (Computerised Imaging Refernce Systems Inc, Norfolk, USA). The CIRS head phantom, in addition to a cavity suitable for gel insertion, contains a bone-equivalent plastic skull and cervical vertebrae, a brain-tissue-equivalent epoxy filling the cranium, air volumes in the nasal cavities and tissue-equivalent epoxy making up the rest of the volume.

Before and after irradiation, the gel container was removed from the phantom, placed in a purpose-built scanning assembly, immersed in a liquid bath and imaged using an Octopus-IQ laser optical CT scanner (MGS Research Inc., Madison, USA). The refractive index of the liqud bath was matched to the refractive index of the central 3 to 3.5 cm of the gel, including the (less than 1 mm thick) container walls on either side. Oblique transmission of the imaging laser through several milimetres of plastic at the container wall produced a localised artefact which appeared as a ring around the gel at the location of the wall. Consequently, this region was excluded from much of the analysis discussed herein. (See publications by Olham *et al* for details regarding the capabilities and limitations of the process of optically scanning dosimetry gels (Oldham et al. 2003, Oldham & Kim 2004, Oldham et al. 2008).) Both scans employed a slice thickness of 0.05 cm and 720 angular projections, and recorded the resulting data in $0.05 \times 0.05 \times 0.05$ cm^3 voxels, giving the three-dimensional image of the irradiated gel sufficient resolution to accurately represent the penumbrae and the details of our small, stereotactic dose distribution. The gel was placed inside the CIRS head phantom, for simulation, treatment planning and irradiation.

The head phantom was CT scanned after positioning using the BrainLab frameless thermoplastic mask and localiser system (BrainLab, Feldkirchen, Germany), allowing the same system to be used to accurately position the phantom for irradiation. The phantom CT scan was imported into the Phantom Mapping module of the BrainLab iPlan treatment plannng system, where a 12 field, non-coplanar, conformal stereotactic radiosurgery treatment was copied from an existing meningioma patient plan and centred on the gel. The targeted lesion in the original plan had a 1.5 cm diameter, and the necessary treatment fields had an average width of 2 cm. The dose was scaled down from the original presciption of 12 Gy in one fraction, to 4 Gy in one fraction, so that the PAGAT gel would not be irradiated beyond its linear response range, and the dose to the phantom was recalculated using the iPlan pencil-beam algorithm.

The treatment was delivered to the head phantom using a Varian iX linear accelerator (Varian Medical Systems, Palo Alto, USA) augmented with a BrainLab m3 micro-multileaf collimator (μMLC). Immediately after irradiation, the gel container was removed from the head phantom and refrigerated at 4^oC. The gel was read out twelve hours after irradiation, as recommended by Venning *et al* (Venning et al. 2005).

Radiation dosimetry gel batches are often calibrated by irradiating a set of small vials of gel to a series of known doses, and thus obtaining a dose-response relationship (Baldock et al. 2010). For PAGAT and other gels, the 'multiple vials' technique has been shown to introduce dose uncertainty, due to the influence of the non-water-equivalent vial walls (Taylor et al. 2007, Taylor et al. 2009*b*). Although the use of independent dosimeters embedded in the gel have been proposed (Poole et al. 2011, Trapp et al. 2009), this study ustilises a simpler technique for calibration of a single gel sample. Given the linear dose-response of PAGAT gel (Venning et al. 2005, DeDeene et al. 2006, Khoei et al. 2010), the measured dose could be straightforwardly normalised using the maximum optical scanner reading obtained at the centre of the irradiated region of the gel. Such self-calibration usually requires an additional low-dose normalisation point, however the PAGAT batch used in this study produced produced a zero optical scanner reading for zero dose, as indicated by profile data shown in Section 3. Similar behaviour has been observed in optically-scanned PAGAT batches that use THPC concentrations above 8 mM (Khoei et al. 2010).

In-house Matlab codes (MathWorks Inc., Massachusetts, USA) were used to produce a three dimensional relative dose distribution by: subtracting the initial gel scan from the irradiated gel scan; reconstructing a series of two-dimensional image slices and assembling the data in a 3D array; and normalising these data using the maximum value found in the central region of the gel. Further Matlab codes were used to rotate the gel dose array, so that it could be registered to iPlan's calculated dose distribution, and to output- two and three-dimensional representations of the gel dose distribution.

TurboReg (Thevenaz et al. 1998) was used as a plugin to ImageJ (U. S. National Institutes of Health, Bethesda, USA) to perform automatic, intensity-based registration of two-dimensional dose images obtained from gel measurement and calculation. Examination of profile data (exemplified in Section 3, suggested that this resulted in

negligible geometric displacement between the images. ImageJ was also used to evaluate the mean dose and the standard deviation from the mean dose in a 0.36×0.36 cm^2 region of interest at the centre of the irradiated volume, to provide an indication of the relative nose in each dataset, so that gamma evaluations performed using MCDTK could use the dose image with the greatest noise as the reference image for all comparisons (Low & Dempsey 2003). MCDTK automatically interpolates between data points, as recommended by Wendling itet al (Wendling et al. 2007), so that the dose distributions could be evaluated using steps less than or equal to one third of the distance-to-agreement criterion. In this case, no interpolation was necessary when evaluating dose distributions using γ(3%,3mm), but all dose distributions required interpolation when evaluated using γ(2%,1mm).

2.2. Monte Carlo simulation

The Monte Carlo simulation of the treatment delivered to the phantom containing the gel was run on a 608-core high performance computing cluster, using the BEAMnrc and DOSXYZnrc codes (Rogers et al. 1995). The BEAMnrc simulations of the radiation beams used a model of the Varian iX linear accelerator and BrainLab m3 μMLC, which has previously been shown (via comparison with radiochromic film) to be capable of accurate simulations of simple micro-collimated test fields (Kairn, Kenny, Crowe, Fielding, Franich, Johnston, Knight, Langton, Schlect & Trapp 2010, Kairn, Aland, Franich, Johnston, Kakakhel, Kenny, Knight, Langton, Schlect, Taylor & Trapp 2010) as well as complex patient treatment fields (Kairn et al. 2011). Input files containing the specific jaw and MLC settings used in each field were automatically produced using Crowe *et al*'s MCDTK (Monte Carlo DICOM ToolKit) code, taking the DICOM-RT export of the iPlan treatment plan as input. The DOZXYZnrc calculations of the dose deposited in the head phantom containing the gel used an 'egsphant', a voxelised model produced from the phantom CT by MCDTK, using density calibration information from the specific CT scanner used.

The twelve beams in the treatment were simulated separately and MCDTK was used to evaluate a weigted sum of the doses, taking into account the number of monitor units per beam as well as the effect of backscatter from the secondary collimators (jaws and μMLC) into the linear accelerator's monitor chamber (Popescu et al. 2005, Kairn et al. 2009). Analysis of the resulting 3ddose file was completed using MCDTK as well as ImageJ.

3. Results

Figure 1 shows transverse slices through the isocentre in the three-dimensional dose distributions obtained from the treatment planning system, gel measurement and Monte Carlo calculation, alongside the corresponding slice from the CT of the head phantom containing the gel. Qualitative comparison of the three dose images shows

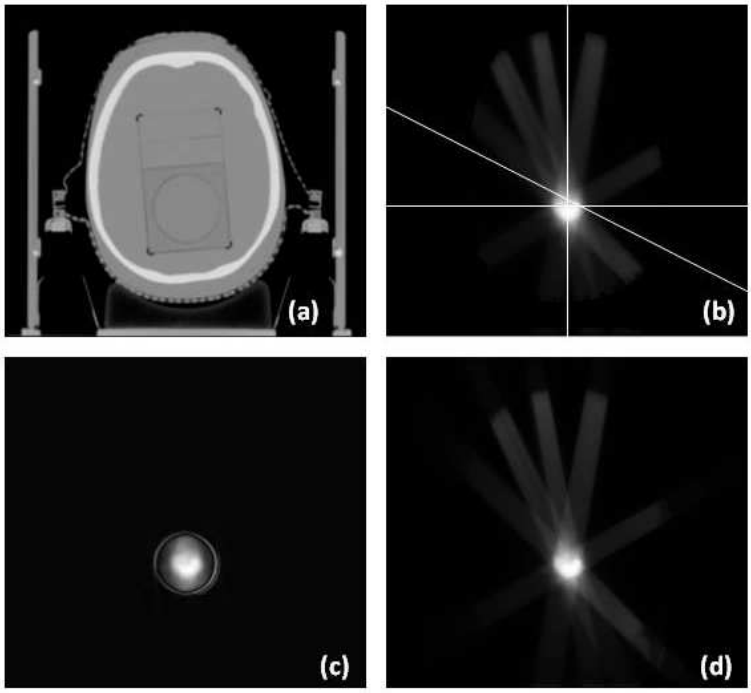

Figure 1. Transverse slices through the isocentre obtained from (a) the CT of the CIRS head phantom containing the gel (circular region, in lower half of image), (b) the three-dimensional dose distribution produced by the iPlan treatment planning system (this figure also shows the positions of the profiles illustrated in Figures 3(a), (b) and (c), as a vertical, horizontal and diagonal line, respectively), (c) the three-dimensional dose distribution obtained from the gel measurement and (d) the three-dimensional dose distribution obtained from the Monte Carlo simulation. Note that in the dose images (b, c and d) lighter pixels represent regions of higer dose, and dose outside the patient is automatically zeroed in the treatment planning system data (b).

general agreement, with the irradiated volume appearing in the same position, with the same general shape, in all three images. Comparison of the dose images from the treatment planning system and Monte Carlo calculations, where the transmission of the beams through the phantom is most apparent, indicates that there was good geometric agreement between the positions, shapes and orientations of the beams that delivered the dose. The ring aound the measurement region in Figure 1(c) provides an indication of the location and intensity of an artefact that affected the accuracy of the gel measurement close to the container walls (described in Section 2.1).

Figure 2(a), (b) and (c) show a set of more quantitative representations of the dose distributions from the three datasets. These figures illustrate the dose within a 3×3 cm^2 region of interest, centred at the isocentre. The maximum dose identified in the gel equates to the maximum dose predicted by the treatment planning system, because it was normalised to do so, and the maximum dose identified in the independent data from the Monte Carlo simulation differs by less than 0.5%. However, there are subtle differences between these three results. Comparison of Figures 2(a) and (b) indicates

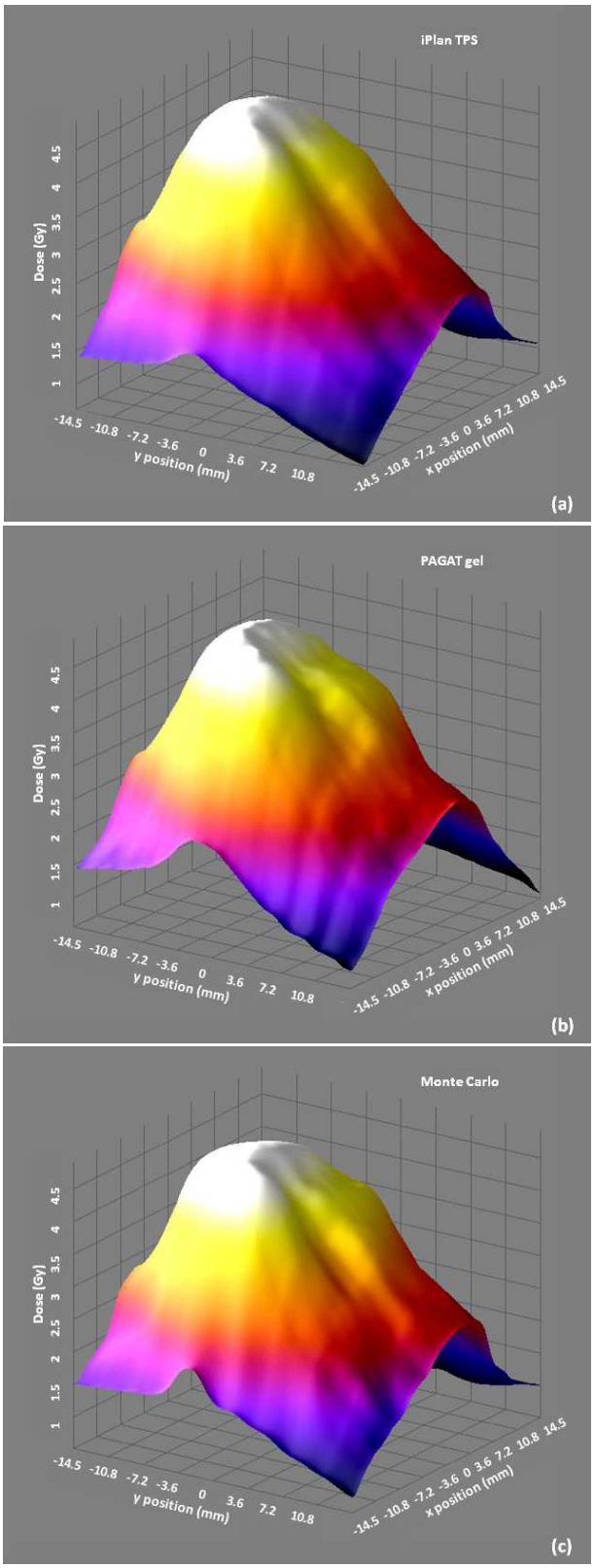

Figure 2. Three dimensional surface plots of the dose in a 3×3 cm^2 region of interest at the treatment isocentre, as (a) predicted by the iPlan treatment planning system, (b) measured using the PAGAT gel and (c) calculated using Monte Carlo simulations.

that the gel has detected small variations, or bumps, in the region around the 4 Gy isodose, which are less apparent in the treatment planning system data. Figure 2(b) suggests that the dose calculated via Monte Carlo simulation confirms this aspect of the gel measurement. By contrast, in the region around $x = 14.5$ cm, near the edge of the field, the dose measured by the gel decreases almost linearly, while the Monte Carlo data in Figure 2(c) show a much shallower rate of decrease in this region.

The standard deviation from the mean dose, calculated as a percentage of the mean dose in a small region at the centre of the irradiated volume (as described in Section 2.1), was found to equate to 0.4% for the Monte Carlo data, 0.5% for the iPlan data and 1.3% for the data obtained from the gel measurement. These results, in addition to providing an indication of the precision of the Monte Carlo dose calculation, provide an indication of the noise level in each of the three data sets, so that gamma evaluations can be performed with the higher-noise dataset taken to be the reference, in order to avoid unerestimation of gamma values (Low & Dempsey 2003).

Gamma evaluations of the data shown in Figures 2(a), (b) and (c), which do not include regions adjacent to the gel container walls, indicate that more than 99% of the values in all three datasets agree with one another within standard acceptance criteria, $\gamma(3\%, 3mm)$. However, when more stingent acceptance criteria, $\gamma(2\%, 1mm)$, are used the proportion of dose values from the gel that agree with the treatment planning dose values decreases to 78%, while the proportion of dose values from the gel that agree with the Monte Carlo dose values remains higher, at 89%. This result provides valuable confirmation that although there are regions where the dose distribution obtained from the gel differs from the treatment planning prediction, the gel measurement is nontheless providing an accurate measurement of the dose, as calculated via Monte Carlo simulations.

Figure 3(a), (b) and (c) show examples of dose profiles evaluated using treatment planning dose calculations, gel measurements and Monte Carlo simulations. In Figure 3(a) it is apparent that the small-scale, local dose variations that were observed in the gel data (Figure 2(b)), at around the 4 Gy isodose, closely match the small dose variations apparent in the Monte Carlo data (Figure 2(c)), in the same region. These small-scale dose variations, which are not predicted by the treatment planning system, may result from contributions to the dose from particularly narrow regions of the treatment beams. Examples of beam's-eye-views shown in Figures 4(a) and (b) indicate that although the plan used in this study was designed to treat a 1.5 cm meningioma with 2 cm beams, avoidance of the brainstem and optic nerves required some fields to be substantially narrowed by the μMLC. The accuracy of the treatment planning system's calculation of dose in these regions may have been compromised by simplistic beam penumbrae modelling as well as the possible inaccuracy of the small field profile measurements used by the planning system.

In Figure 3(a), it is apparent that the reliability of the gel measurement breaks down in the regions close to the container walls (at positions + and - 2.1 cm), where the measured dose falls precipitously to zero while the dose calculated by both the

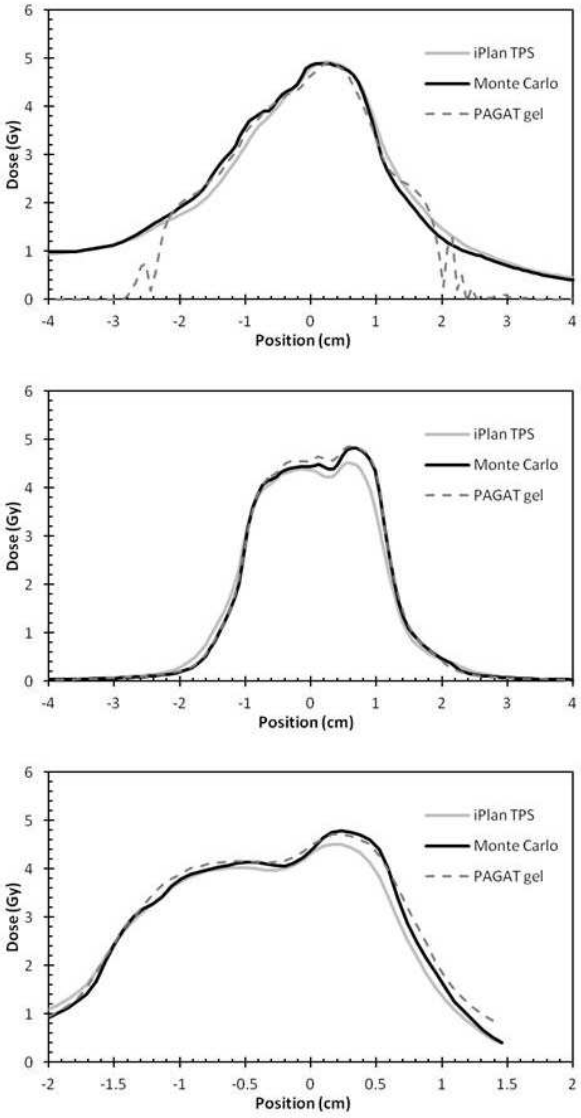

Figure 3. Dose profiles through different regions in the dose distribution. Profiles (a) and (b) pass through the isocentre, while profile (c) is oblique and off-axis. The locations at which these profiles were obtained is indicated in Figure 1(b).

treatment planning system and the Monte Carlo simulations remain above 1 Gy. The same behaviour is not observed in Figure 3(b) because the dose in this direction decreases to close to zero before the walls are approached.

Figure 3(b) illustrates a set of profiles through the three dose distributions in a region where the beam penumbrae are narrow. Analysis of the data used to generate these profiles indicates that the gel and Monte Carlo data agree in indicating that the penumbra width, measured as the distance between the 80% and 20% isodoses, is 3 mm narrower (on the positive side of the profile) than the treatment planning system predicts.

Figure 3(c) provides a worst-case-scanario, indicating that there are some regions

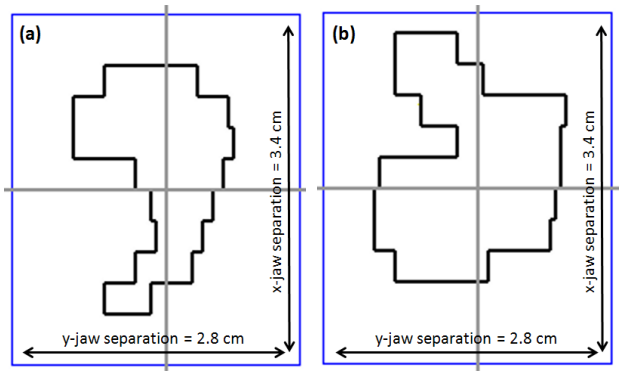

Figure 4. Beam's-eye-view diagrams of two of the twelve fields that contributed to the treatment. The beam orientations (gantry, floor, collimator) were (a) (285, 300, 60) and (b) (330, 270, 90).

where the Monte Carlo calculation results provide a better match with the treatment planning data than with the gel measurement data. Even in these profiles, however, it is evident that the Monte Carlo generally confirm the gel measurements, rather than duplicating the treatment planning predictions.

4. Conclusion

In this study a small volume of PAGAT gel in a heterogeneous head phantom was used to provide a high-resolution measurement of the dose delivered during a stereotactic radiosurgery treatment. The accuracy of the dose measured in the gel was examined via comparison with a detailed Monte Carlo simulation of the treatment to the phantom and gel. The dose distributions obtained from Monte Carlo and from the gel measurement were found to be in better agreement with each other than with the dose distribution provided by the treatment planning system's pencil-beam calculation. Both sets of data showed close agreement with the treatment planning system's dose distribution through the centre of the irradiated volume, but both the gel and the Monte Carlo dose distributions also showed increased sensitivity to the effects of density heterogeneities and measured narrower beam penumbrae than was observed in the treatment planning system's predicted dose distribution.

The Monte Carlo simulations allowed the accuracy of the PAGAT gel dosimeter to be verified in this case, allowing PAGAT gel to be utilised in the measurement of dose from stereotactic and other radiotherapy treatments, with greater confidence in the future.

Acknowledgments

SBC's contribution to this study was supported by the Australian Research Council, the Wesley Research Institute, Premion and the Queensland University of Technology

(QUT), through linkage grant number LP110100401. MLT's contribution to this work was funded by the NHMRC, Australia (grant number 555420). MLT and RDF's travel between Melbourne and Brisbane was funded by the Wesley Research Institute (grant number 2008/11). Computational resources and services used in this work were provided by the HPC and Research Support Unit, QUT. Access to QUT HPC facilities and optical gel scanning equipment was provided by the Queensland Cancer Physics Collaborative.

References

Baldock C, DeDeene Y, Doran S, Ibbott G, Jirasek A, Lepage M, McAuley K B, Oldham M & Schreiner L J 2010 *Physics in Medicine and Biology* **55**, R1–R63.

Boudou C, Biston M C, Corde S, Adam J F, Ferrero C, Esteve F & Elleaume H 2004 *Physics in Medicine and Biology* **49**, 5135–5144.

Boudou C, Tropres I, Rousseau J, Lamalle L, Adam J F, Esteve F & Elleaume H 2007 *Physics in Medicine and Biology* **52**, 4881–4892.

Calcina C S G, deOliveira L N, deAlmeida C E & deAlmeida A 2007 *Physics in Medicine and Biology* **52**, 1431–1439.

Ceberg S, Gagne I, Gustafsson H, Scherman J B, Korreman S S, Kjr-Kristoffersen F, Hilts M & Back S A J 2010 *Physics in Medicine and Biology* **55**, 4885–4898.

Cosgrove V, Murphy P, McJury M, Adams E, Warrington A, Leach M & Webb S 2000 *Physics in Medicine and Biology* **45**, 11951210.

Das I J, Ding G X & Ahnesjo A 2008 *Medical Physics* **35**(1), 206–215.

DeDeene Y, Vergote K, Claeys C & DeWagter C 2006 *Physics in Medicine and Biology* **51**, 653–673.

Guillerminet C, Gschwind R, Makovicka L, Spevacek V, Soukoup M & Novotny J 2005 *Radiation Measurements* **39**, 39–42.

Kairn T, Aland T, Franich R D, Johnston P N, Kakakhel M B, Kenny J, Knight R, Langton C M, Schlect D, Taylor M L & Trapp J V 2010 *Physics in Medicine and Biology* **55**(17), N451–N463.

Kairn T, Crowe S B, Kenny J & Trapp J V 2011 *Radiation Measurements* **46**(12), 1985–1988.

Kairn T, Crowe S B, Poole C M & Fielding A L 2009 *Australasian Physical and Engineering Sciences in Medicines* **32**(3), 129–135.

Kairn T, Kenny J, Crowe S B, Fielding A L, Franich R D, Johnston P N, Knight R T, Langton C M, Schlect D & Trapp J V 2010 *Medical Physics* **37**(4), 1761–1767.

Khoei S, Moorrees J B, Langton C M & Trapp J V 2010 *Journal of Physics Conference Series* **250**, 012019.

Low D A & Dempsey J F 2003 *Medical Physics* **30**(9), 2455–2464.

Oldham M & Kim L 2004 *Medical Physics* **31**, 1093–1104.

Oldham M, Sakhalkar H, Guo P & Adamovics J 2008 *Medical Physics* **35**, 2072–2080.

Oldham M, Siewerdsen J H, Kumar S, Wong J & Jaffray D A 2003 *Medical Physics* **30**, 623–634.

Pappas E, Seimenis I, Angelopoulos A, Georgolopoulou P, Kamariotaki-Paparigopoulou M, Maris T, Sakelliou L, Sandilos P & Vlachos L 2001 *Physics in Medicine and Biology* **46**, 783–797.

Poole C M, Trapp J V, Kenny J, Kairn T, Williams K, Taylor M, Franich R & Langton C M 2011 *Australasian Physical and Engineering Sciences in Medicine* **34**(3), 327–332.

Popescu I A, Shaw C P, Zavgorodni S F & Beckham W A 2005 *Physics in Medicine and Biology* **50**(14), 3375–3392.

Pourfallah T A, Allahverdi M, Alam N R, Ay M R & Zahmatkesh M H 2009 *Medical Physics* **36**, 3002–3012.

Rogers D W O, Faddegon B A, Ding G X, Ma C M & We J 1995 *Medical Physics* **22**, 503–524.

Seimenis I, Moutsatsos A, Petrokokkinos L, Kantemiris I, Benekos O, Efstathopoulos E, Papagiannis P, Spevacek V, Semnickae J & Dvorak P 2009 *Journal of Instrumentation* **4**, P07004.

Taylor M L, Franich R D, Trapp J V & Johnston P N 2008 *Australasian Physical and Engineering Sciences in Medicine* **31**, 131–138.

Taylor M L, Franich R D, Trapp J V & Johnston P N 2009*a* *Radiation Research* **171**, 123–125.

Taylor M L, Franich R, Johnston P N, Miller M & Trapp J V 2007 *Physics in Medicine and Biology* **52**, 3991–4005.

Taylor M L, Franich R, Trapp J V & Johnston P N 2009*b* *IEEE Transactions on Nuclear Science 56(2): 429-436.* **56**(2), 429–436.

Taylor M L, Kron T & Franich R D 2011 *Acta Oncologica* **50**, 483508.

Thevenaz P, Ruttimann U E & Unser M 1998 *IEEE Transactions on Image Processing* **7**(1), 27–41.

Trapp J V, Kairn T, Crowe S & Fielding A 2009 *Journal of Physics: Conference Series* **164**, 012014.

Valente M, Aon E, Brunetto M, Castellano G, Gallivanone F & Gambarini G 2007 *Nuclear Instuments and Methods in Physics Research, A* **580**, 497–501.

Venning A J, Hill B, Brindha S, Healy B J & Baldock C 2005 *Physics in Medicine and Biology* **50**, 3875–3888.

Wendling M, Zijp L J, McDermott L N, Smit E J, Sonke J J, Mijnheer B J & vanHerk M 2007 *Medical Physics* **34**(5), 1647–1654.